Editors' Suggestion

Alternative Frictional Model for Discontinuous Shear Thickening of Dense Suspensions: Hydrodynamics

Safa Jamali[1] and John F. Brady[2]
[1]Mechanical and Industrial Engineering Department, Northeastern University, Boston, Massachusetts 02115, USA
[2]Division of Chemistry and Chemical Engineering, California Institute of Technology, Pasadena, California 91125, USA

(Received 2 May 2019; revised manuscript received 24 July 2019; published 25 September 2019)

A consensus has emerged that a constraint to rotational or sliding motion of particles in dense suspensions under flow is the genesis of the discontinuous shear thickening (DST) phenomenon. We show that tangential fluid lubrication interactions due to finite-sized asperities on particle surfaces effectively provide these constraints, changing the dynamics of particle motion. By explicitly resolving for the surface roughness of particles, we show that, while smooth particles exhibit continuous shear thickening, purely hydrodynamic interactions in rough particles result in DST. In contrast to the frictional contact model, the hydrodynamic model predicts negative first and second normal stress differences for dense suspensions in the shear thickened state.

DOI: 10.1103/PhysRevLett.123.138002

Main.—From a rheological standpoint, material functions (viscosity and normal stress differences) of dense suspensions under shear show distinct non-Newtonian behavior. Upon increasing the rate of applied deformation, the viscosity of a dense suspension may increase incrementally or abruptly, respectively, corresponding to continuous (CST) and discontinuous shear-thickening (DST) behavior [1–3]. A number of experimental studies [4–7] suggest that both the first and second normal stress differences, N_1 and N_2, are negative in sign, and comparable in magnitude for shear-thickening suspensions. In contrast, a number of recent experiments show a sign reversal in N_1 for DST suspensions [8–12], which does not necessarily coincide with a transition in the viscosity. The breadth of macroscopic rheological response in dense suspensions to an applied deformation has stimulated decades of research in the rheology and physics community alike; yet, the topic has become most debated during the past few years. We present a very brief history of the topic in order to put the recent developments in context.

During mid-20th century, dilatancy and shear thickening were used interchangeably to describe the same rheological behavior [13–15]; however, dilatancy is the volume expansion in sheared dense suspensions, not the increase in viscosity. Another suggested mechanism for shear thickening (ST) in dense suspensions at the time was an order-disorder transition as the stringlike ordered structures in the shear thinning regime are disrupted at higher shear rates [14]. Later, development of a computational platform based on hydrodynamics of suspensions under shear [16–19] suggested that dissipative lubrication forces in small interparticle gaps give rise to the formation of so-called hydroclusters that resist large deformations and in turn increase the viscosity [2,20–24]: the lubrication stresses scale inversely with the surface-surface separation distance between the colloidal particles $1/h$, and thus in principle are infinite at contact. This, in other words, means that hard spheres never contact one another; however, this also means that as suspensions get denser, the smaller gaps result in larger stresses. Since lubrication forces are naturally dissipative and act against the relative motion of particles, they provide a natural rate dependence for the macroscopic rheology of suspensions. This motivated presentation of viscometric functions as a function of the Peclet number, $\mathrm{Pe} = 6\pi\eta_0\dot{\gamma}R^2/(k_BT/R)$ (η_0 is the suspending fluid viscosity, $\dot{\gamma}$ is the imposed shear rate, and R is the particle radius), which represents the relative magnitude of shear forces to Brownian forces. Through a series of micromechanical studies, it has been [25–31] suggested that since the normal direction of the squeezing mode lubrication scales as $1/h$ and the tangential direction scales as $\log(1/h)$, neglecting such tangential interactions does not significantly change the macroscopic rheology recovered by the model. This picture of the colloidal hydrodynamics has been employed in describing rheology of not only hard sphere suspensions, but also suspensions of soft particles [20], cubic particles [32], and the microstructural evolutions under shear [33]. Additionally, the microstructures produced via Stokesian dynamics simulations [23,24] show a remarkable agreement with experimentally observed structures through scattering experiments [21,34,35]. While the hydrodynamics-based mechanism recovers a negative N_1 in ST, it fails to reproduce the DST behavior and only an intermediate CST increase to viscosity (three- to sixfold) is predicted. On the other hand, careful experiments performed on particles with tunable

roughness [8,36] showed that one can transition from CST to DST by systematically changing the surface definition of the particles. A series of flow reversal [37] as well as orthogonally superposed oscillatory deformations [38] called into question whether hydrodynamic interaction are sufficient in reproducing DST behavior. These recent developments, as well as a constraint-based approach to DST presented recently by Guy *et al.* [39] confirm that a single normal mode of dissipation cannot explain the whole ST phenomenon, and a so-called rolling constraint is essential in order to reduce a particle's degrees of freedom and generate stresses relevant to DST. Over the past few years, a general consensus has emerged [36,40–43], proposing a frictional contact mechanism for ST in dense suspensions: the lubrication layer breaks down under large deformation rates and upon contact between the particles, a Coulomb's law of friction determines whether the particles stick or slip. The frictional contact model successfully recovers the DST behavior; however, the tangential nature of frictional interactions results in a consistent positive N_1 value [8,41,42,44]. Furthermore, a recent work by Townsend and Wilson [45] introducing the role of surface roughness using a combination of frictional contact model and Stokesian dynamics clearly showed that particle-particle overlaps are essential in recovering large viscosities in the DST regime.

Here we present an alternative underpinning to sliding motion of particles based purely on hydrodynamic interactions, where a more realistic picture of the particle surface is used. Perhaps a major shortcoming of the lubrication theory in explaining the DST is the smooth hard-sphere assumption: In real life there is no perfect hard sphere. Ultimately, particles have different levels of asperities on their surface, with a finite mean square roughness value. Although the normal squeezing mode lubrication dominates the motion of particles in small gaps, when the separation distance is comparable with the size of asperities, the lubrication due to interaction of asperities can no longer be ignored and the resulting forces and motion of particles no longer need to be along the center-center line of the two particles. The bottom row images in Fig. 1 show an example of the particle-particle spacing in small gaps: h for the surface separation of two primary base particles, and h' for the separation of their corresponding asperities. The tangential lubrication stresses for smooth surfaces scale as $\propto \log(1/h)$, while the normal lubrication stresses between the asperities scale $\propto 1/h'$ (note that $h > h'$). In other words, the dominant forces defining the motion of particles are now the hydrodynamic interactions between surface asperities rather than between the primary base particles themselves. The normal lubrication forces of asperities translate into tangential forces and hence a torque on the particle. Thus, in our model the tangential lubrication forces of the base particles as well as the asperities are neglected, and the tangential motion or hindrance results solely from the normal squeezing mode lubrication between the asperities.

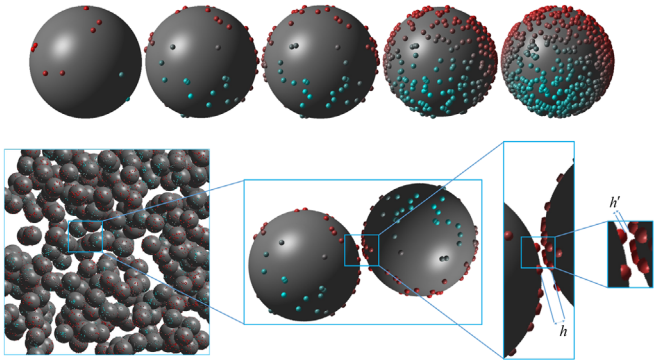

FIG. 1. Top row: increasing surface coverage from 0.01 to 0.5 by the same size asperities, and bottom row: depiction of particle-particle separation in close contact.

In order to include such effects, we introduce a simulation scheme based on dissipative particle dynamics (DPD) [20,46], for rough composite colloids interacting hydrodynamically. In our DPD scheme, the equation of motion for all particles is written as $m_i \frac{d\mathbf{v}_i}{dt} = \sum \mathbf{F}_{ij}^C + \mathbf{F}_{ij}^D + \mathbf{F}_{ij}^R + \mathbf{F}_{ij}^H + \mathbf{F}_{ij}^{\mathrm{Rep}}$, where each term on the right-hand side represents a pairwise interaction potential between the ith particle and any neighboring jth particles. The solvent is explicitly modeled as soft particles, interacting through the first 3 terms: The conservative force $\mathbf{F}_{ij}^C$ is exclusively used for the solvent based on the chemical identity of the interacting species, which is parametrized based on the compressibility of water [47]; the random force $\mathbf{F}_{ij}^R$ introducing the Brownian thermal fluctuations in the system using a random function Θ_{ij} of a zero mean and a unit variance; and the dissipative force $\mathbf{F}_{ij}^D$ that acts as the heat sink and dissipates the generated heat of the random force used in equations of motion for both colloids and the solvent. The random and dissipative forces are thus coupled and satisfy the fluctuation-dissipation theorem [48] and provide the canonical ensemble required for proper representation of Brownian forces in the system. The remaining terms are calculated only for the colloidal particles: the hydrodynamic forces $\mathbf{F}_{ij}^H$ and the interparticle forces $\mathbf{F}_{ij}^{\mathrm{Rep}}$. The hydrodynamic force, $\mathbf{F}_{ij}^H = -\mu_{ij}^H(\mathbf{v}_{ij}.\mathbf{e}_{ij})\mathbf{e}_{ij}$ (where $\mathbf{e}_{ij}$ is the unit normal vector, and $\mathbf{v}_{ij}$ is the relative velocity between particles), represents the short-ranged lubrication forces based on the pair drag term, $\mu_{ij}^H = 3\pi\eta_0 a_1 a_2/2h_{ij}$, in squeeze mode [27], which diverges at the surface-surface contact point, $h_{ij} = 0$. Here,a_1 and a_2 are the radii of the interacting colloids and η_0 is the viscosity of the suspending fluid. It should be noted that the hydrodynamic interactions are calculated for asperity-asperity and base-base interactions, and neglected for asperity-base interactions as the pair drag assumption breaks down for large particle size ratios and those lubrication interactions are significantly

weaker than the same size pair drag terms. Furthermore, since in DPD formalism the explicit representation of solvent particles ensures preservation of hydrodynamics, $\mathbf{F}_{ij}^{H}$ is only invoked when the distance between two colloidal particles is smaller than a single solvent particle, i.e., upon break down of the DPD hydrodynamics [20,44,46]. We regularize the singularity of the pair drag term at a small separation, $\delta = 10^{-4}a$. The repulsive force, $\mathbf{F}_{ij}^{\mathrm{Rep}} = F_0 e^{-\kappa h}.\mathbf{e}_{ij}$, represents the electrostatic double-layer force between the colloidal particles, and is a short-ranged interaction potential vanishing exponentially at $\kappa^{-1} = 0.01a$ distance. In this work we choose a constant value of $F_0 = 10^3\ k_B T/a$ for the repulsion in between the base colloidal particles. The asperity-asperity repulsion interactions are intentionally ignored here to avoid a long-range frictionlike effect arising. Each colloidal particle is a composite construction of a base particle decorated with small spheres with their center located at the surface of the base particles, with a rigid body dynamic. The stress tensor is calculated using an Irving-Kirkwood [49,50] formalism, based on individual particle velocities, and each of the interactions acting in between pairs of particles, $\boldsymbol{\sigma} = (1/V)\{\sum_{i=1}^{N} m_i[\mathbf{v}_i - \mathbf{u}(r_i)] \otimes [\mathbf{v}_i - \mathbf{u}(r_i)] + \sum_{j>i}^{N}\sum_{i=1}^{N-1} \mathbf{r}_{ij} \otimes \mathbf{F}_{ij}\}$, where V is the total volume of the calculation box, and $\mathbf{u}(r_i)$ is the stream velocity on the position of the particle across the velocity gradient direction.

Composite geometries were made from base particles of radius a, and asperities of size $b = 0.05\ a$ as shown in Fig. 1. There are multiple ways for changing the root mean square roughness of a particle decorated with smaller spheres, by changing the decoration pattern, size of the asperities, and the number of asperities. Here, we use the total coverage of the base particle surface by monodispersed spherical asperities as a measure of roughness (asperity centers are randomly placed on the surface of base particles). Simulations are performed on 1000 base particles (for $\phi = 0.58$), with the number of asperities varying from 10 (~0.01 surface coverage) to 500 (~0.5 surface coverage) per base particle (shown in Fig. 1 top row), with the total number density of 3.0 for solvent particles and dimensionless temperature of $k_B T = 1$. Bimodality of the primary colloidal particles is introduced to avoid order formation, by a volumetric ratio of 1:1 of larger colloidal particles with $a' = 1.4\ a$. Since the length scale is set by the smaller asperities in our simulations, small time steps of $\Delta t = 10^{-7}\ a(m/k_B T)^{0.5}$ were taken in order to minimize the overlap events between the colloidal particles, where m is the mass of a single DPD particle.

General flow curves of the suspensions at different fractions of solid particles, and over a range of different asperity-covered surface area are presented in Fig. 2. While at intermediate volume fraction of $\phi = 0.35$, introduction of surface roughness does not change the viscosity of

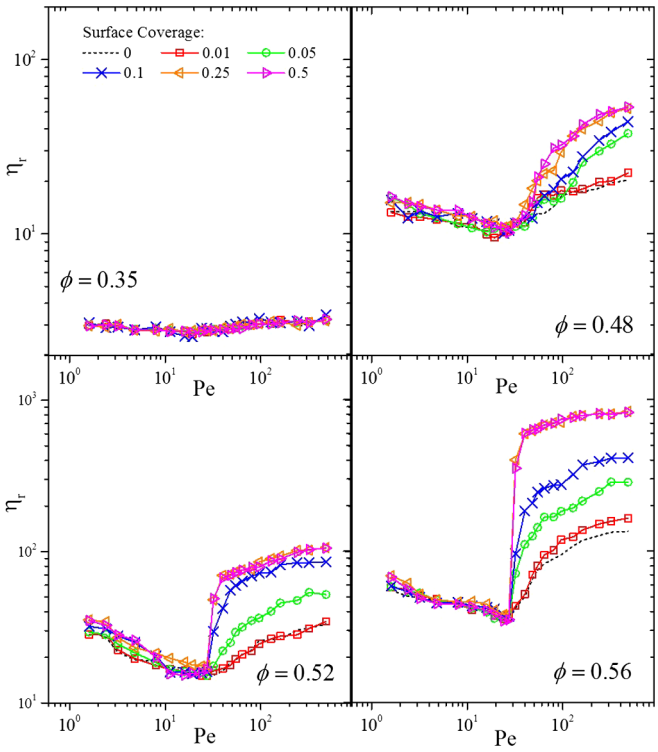

FIG. 2. Relative viscosity against the Peclet number for a range of different volume fractions ($\phi = 0.35$, 0.48, 0.52, 0.56) and surface area covered by the asperities.

suspensions, increasing the volume fraction to $\phi = 0.48$ strengthens the shear thickening for particles with higher surface coverage. At higher volume fractions of $\phi = 0.52$, 0.56 this clearly results in a transition from CST to DST behavior as surface roughness is increased to 0.25; however, increasing the surface coverage from 0.25 to 0.5 does not change the overall viscosity and shear stress. Regardless of the evident changes in the shear-thickened state viscosity and increase of the viscosity in general, changing the surface definition of the particles does not change the shear-thinning behavior of the suspensions over the range of parameters studies, nor the onset of ST. Previous studies have shown that the onset of ST is effectively set by the repulsive interactions in between the particles F_0 [44,51]. Results here are very similar in comparison to the Stokesian dynamics simulations of frictional particles by Mari and co-workers [41,42], with a fundamental difference: in the frictional contact model the stresses are generated through particle-particle contacts, unlike the purely hydrodynamic stresses in our model where stresses are born in fluid phase and through small gaps in between surface asperities.

With directions of flow, velocity gradient, and vorticity defined as 1, 2, and 3, respectively, the first, $N_1 = \sigma_{11} - \sigma_{22}$, and second, $N_2 = \sigma_{22} - \sigma_{33}$, normal stress differences normalized by the Newtonian fluid stress, $\sigma_f = \eta_0 \dot{\gamma}$ as a function of dimensionless Peclet number are

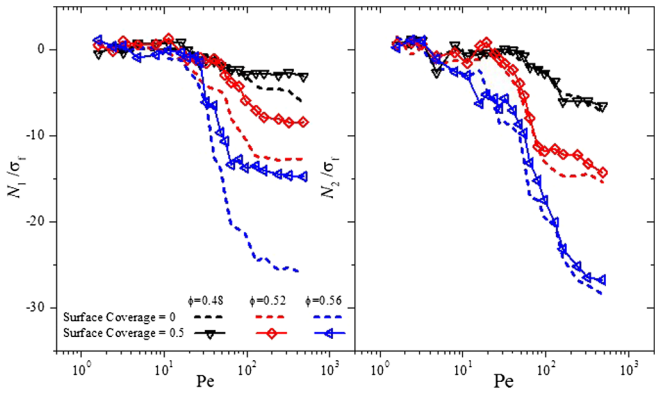

FIG. 3. First (left) and second (right) normal stress differences normalized by the fluid stress, against the applied Peclet number for a range of different volume fraction of particles, and for smooth and rough particles.

presented in Fig. 3 for two cases of smooth and rough particles. In contrast to the first normal stresses predicted by the frictional contact model [41,44], the normal stress differences predicted by our model are generally negative in sign and large in magnitude. This is in qualitative agreement with experimental measurements of Cwalina and Wagner [7] for shear thickening silica suspensions of similar volume fractions. While N_2 for shear thickening suspensions is consistently negative, the negative sign of N_1 is a hallmark of hydrodynamic stresses [23].

As proposed by Wyart and Cates [40], the maximum packing fraction of colloids in the shear thickened state decreases as rotational motion of particles becomes increasingly hindered. We fit the relative viscosities of smooth and rough particles in the shear-thickened state (at the highest Peclet numbers investigated in Fig. 2, as for some volume fractions a clear ST state plateau is not observed) to a simple empirical model, $\eta_r = C(1-\phi/\phi_{\mathrm{Max.}})^{-\alpha}$ with $\alpha = 2.4$, and the results are shown in Fig. 4. The maximum packing fraction of solid particles evidently decreases from $\phi_{\mathrm{Max}} = 0.62$ for the smooth particles to $\phi_{\mathrm{Max}} = 0.58$ for the particles with 50% coverage of their area.

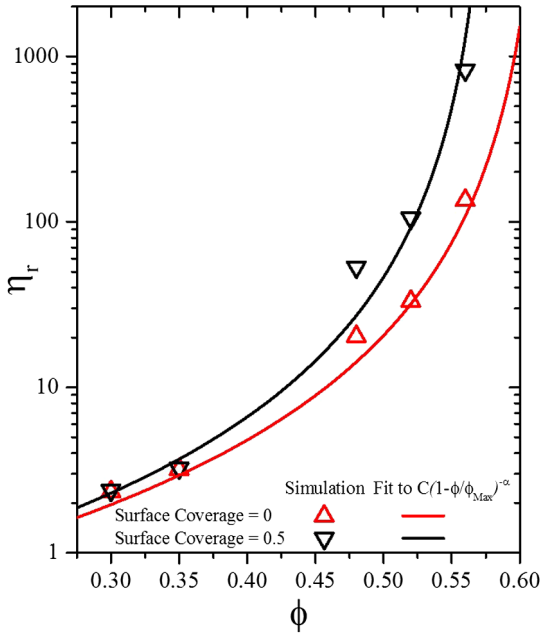

FIG. 4. Relative viscosity versus the fraction of colloidal particles, presented for smooth and rough particles.

In summary we have shown that a detailed resolution of hydrodynamic stresses can reproduce key features of dense suspensions in the shear thickening regime. This further confirms that in order to recover the DST behavior, constraining the rotational (and/or sliding) motion of particles through tangential forces between particles is essential; however, we have shown here that such rolling constraints can be introduced solely by hydrodynamic interactions. Our results give virtually the same viscosities in both the CST and DST regimes, as well as the maximum packing fractions, as those predicted by a frictional contact model. However, in our hydrodynamic model stresses are borne by the fluid (hydrodynamics) and the model predicts negative first and second normal stress differences in the shear thickened state. These results strongly suggest that while particle-particle contacts in fact occur in dense suspensions [52] and frictional forces emerge, such a frictional scenario is merely one mechanism for generating the large stresses required to observe DST. The important physics that leads to DST is the restriction of tangential motion (both sliding and rotation) and our work shows that hydrodynamics alone for rough particles is fully sufficient for generating such restrictions, similar to frictional contacts. An accurate solution to the lubrication interactions between two asperities, the asperity-base particle interactions, as well as underlying physics of shear reversal or superposed oscillatory shear protocols warrant further examination.

[1] J. Mewis and N. J. Wagner, *Colloidal Suspension Rheology*, Cambridge Series in Chemical Engineering (Cambridge University Press New York 2012).
[2] N. J. Wagner and J. F. Brady, Shear thickening in colloidal dispersions, Phys. Today **62**, No. 10, 27 (2009).
[3] E. Brown and H. M. Jaeger, Shear thickening in concentrated suspensions: Phenomenology, mechanisms and relations to jamming, Rep. Prog. Phys. **77**, 046602 (2014).
[4] H. M. Laun, Normal stresses in extremely shear thickening polymer dispersions, J. Non-Newtonian Fluid Mech. **54**, 87 (1994).
[5] M. Lee, M. Alcoutlabi, J. J. Magda, C. Dibble, M. J. Solomon, X. Shi, and G. B. McKenna, The effect of the shear-thickening transition of model colloidal spheres on the sign of N1 and on the radial pressure profile in torsional shear flows, J. Rheol. **50**, 293 (2006).

[6] B. K. Aral and D. M. Kalyon, Viscoelastic material functions of noncolloidal suspensions with spherical particles, J. Rheol. **41**, 599 (1997).
[7] C. D. Cwalina and N. J. Wagner, Material properties of the shear-thickened state in concentrated near hard-sphere colloidal dispersions, J. Rheol. **58**, 949 (2014).
[8] L. C. Hsiao, S. Jamali, E. Glynos, P. F. Green, R. G. Larson, and M. J. Solomon, Rheological State Diagrams for Rough Colloids in Shear Flow, Phys. Rev. Lett. **119**, 158001 (2017).
[9] J. R. Royer, D. L. Blair, and S. D. Hudson, Rheological Signature of Frictional Interactions in Shear Thickening Suspensions, Phys. Rev. Lett. **116**, 188301 (2016).
[10] Y. Madraki, G. Ovarlez, and S. Hormozi, Transition from Continuous to Discontinuous Shear Thickening: An Excluded-Volume Effect, Phys. Rev. Lett. **121**, 108001 (2018).
[11] D. Lootens, H. van Damme, Y. Hémar, and P. Hébraud, Dilatant Flow of Concentrated Suspensions of Rough Particles, Phys. Rev. Lett. **95**, 268302 (2005).
[12] Z. Pan, H. de Cagny, M. Habibi, and D. Bonn, Normal stresses in shear thickening granular suspensions, Soft Matter **13**, 3734 (2017).
[13] A. B. Metzner and M. Whitlock, Flow behavior of concentrated (dilatant) suspensions, Trans. Soc. Rheol. **2**, 239 (1958).
[14] R. L. Hoffman, Discontinuous and dilatant viscosity behavior in concentrated suspensions. I. Observation of a flow instability, Trans. Soc. Rheol. **16**, 155 (1972).
[15] H. A. Barnes, Shear-thickening ("dilatancy") in suspensions of nonaggregating solid particles dispersed in Newtonian liquids, J. Rheol. **33**, 329 (1989).
[16] G. Bossis and J. F. Brady, Dynamic simulation of sheared suspensions. I. General method, J. Chem. Phys. **80**, 5141 (1984).
[17] G. Bossis and J. F. Brady, The rheology of Brownian suspensions, J. Chem. Phys. **91**, 1866 (1989).
[18] G. Bossis, J. F. Brady, and C. Mathis, Shear-induced structure in colloidal suspensions I. Numerical simulation, J. Colloid Interface Sci. **126**, 1 (1988).
[19] J. F. Brady and G. Bossis, The rheology of concentrated suspensions of spheres in simple shear flow by numerical simulation, J. Fluid Mech. **155**, 105 (1985).
[20] S. Jamali, A. Boromand, N. Wagner, and J. Maia, Microstructure and rheology of soft to rigid shear-thickening colloidal suspensions, J. Rheol. **59**, 1377 (2015).
[21] B. J. Maranzano and N. J. Wagner, Flow-small angle neutron scattering measurements of colloidal dispersion microstructure evolution through the shear thickening transition, J. Chem. Phys. **117**, 10291 (2002).
[22] J. Bergenholtz, J. F. Brady, and M. Vicic, The non-Newtonian rheology of dilute colloidal suspensions, J. Fluid Mech. **456**, 239 (2002).
[23] D. R. Foss and J. F. Brady, Structure, diffusion and rheology of Brownian suspensions by Stokesian dynamics simulation, J. Fluid Mech. **407**, 167 (2000).
[24] D. R. Foss and J. F. Brady, Brownian dynamics simulation of hard-sphere colloidal dispersions, J. Rheol. **44**, 629 (2000).
[25] L. E. Silbert, J. R. Melrose, and R. C. Ball, Colloidal microdynamics: Pair-drag simulations of model-concentrated aggregated systems, Phys. Rev. E **56**, 7067 (1997).
[26] L. E. Silbert, J. R. Melrose, and R. C. Ball, The rheology and microstructure of concentrated, aggregated colloids, J. Rheol. **43**, 673 (1999).
[27] R. C. Ball and J. R. Melrose, Lubrication breakdown in hydrodynamic simulations of concentrated colloids, Adv. Colloid Interface Sci. **59**, 19 (1995).
[28] J. R. Melrose and R. C. Ball, The pathological behaviour of sheared hard spheres with hydrodynamic interactions, Europhys. Lett. **32**, 535 (1995).
[29] S. Kim and S. J. Karrila, *Microhydrodynamics: Principles and Selected Applications. Mineola*, (Dover Publication, Inc., New York 1991).
[30] D. J. Jeffrey, The calculation of the low Reynolds number resistance functions for two unequal spheres, Phys. Fluids A **4**, 16 (1992).
[31] D. J. Jeffrey and Y. Onishi, Calculation of the resistance and mobility functions for two unequal rigid spheres in low-Reynolds-number flow, J. Fluid Mech. **139**, 261 (1984).
[32] C. D. Cwalina, K. J. Harrison, and N. J. Wagner, Rheology of cubic particles suspended in a Newtonian fluid, Soft Matter **12**, 4654 (2016).
[33] E. Nazockdast and J. F. Morris, Effect of repulsive interactions on structure and rheology of sheared colloidal dispersions, Soft Matter **8**, 4223 (2012).
[34] R. L. Hoffman, Explanations for the cause of shear thickening in concentrated colloidal suspensions, J. Rheol. **42**, 111 (1998).
[35] H. M. Laun, R. Bung, S. Hess, W. Loose, O. Hess, K. Hahn, E. Hiidicke, R. Hingmann, F. Schmidt, and P. Lindner, Rheological and small angle neutron scattering investigation of shear-induced particle structures of concentrated polymer dispersions submitted to plane Poiseuille and Couette flow, J. Rheol. **36**, 743 (1992).
[36] N. Fernandez, R. Mani, D. Rinaldi, D. Kadau, M. Mosquet, H. Lombois-Burger, J. Cayer-Barrioz, H. J. Herrmann, N. D. Spencer, and L. Isa, Microscopic Mechanism for Shear Thickening of Non-Brownian Suspensions, Phys. Rev. Lett. **111**, 108301 (2013).
[37] N. Y. C. Lin, B. M. Guy, M. Hermes, C. Ness, J. Sun, W. C. K. Poon, and I. Cohen, Hydrodynamic and Contact Contributions to Continuous Shear Thickening in Colloidal Suspensions, Phys. Rev. Lett. **115**, 228304 (2015).
[38] N. Y. C. Lin, C. Ness, M. E. Cates, J. Sun, and I. Cohen, Tunable shear thickening in suspensions, Proc. Natl. Acad. Sci. U.S.A. **113**, 10774 (2016).
[39] B. M. Guy, J. A. Richards, D. J. M. Hodgson, E. Blanco, and W. C. K. Poon, Constraint-Based Approach to Granular Dispersion Rheology, Phys. Rev. Lett. **121**, 128001 (2018).
[40] M. Wyart and M. E. Cates, Discontinuous Shear Thickening without Inertia in Dense Non-Brownian Suspensions, Phys. Rev. Lett. **112**, 098302 (2014).
[41] R. Mari, R. Seto, J. F. Morris, and M. M. Denn, Shear thickening, frictionless and frictional rheologies in non-Brownian suspensions, J. Rheol. **58**, 1693 (2014).
[42] R. Seto, R. Mari, J. F. Morris, and M. M. Denn, Discontinuous Shear Thickening of Frictional Hard-Sphere Suspensions, Phys. Rev. Lett. **111**, 218301 (2013).
[43] C. Heussinger, Shear thickening in granular suspensions: Interparticle friction and dynamically correlated clusters, Phys. Rev. E **88**, 050201(R) (2013).

[44] A. Boromand, S. Jamali, B. Grove, and J. M. Maia, A generalized frictional and hydrodynamic model of the dynamics and structure of dense colloidal suspensions, J. Rheol. **62**, 905 (2018).
[45] A. K. Townsend and H. J. Wilson, Frictional shear thickening in suspensions: The effect of rigid asperities, Phys. Fluids **29**, 121607 (2017).
[46] S. Jamali, M. Yamanoi, and J. Maia, Bridging the gap between microstructure and macroscopic behavior of monodisperse and bimodal colloidal suspensions, Soft Matter **9**, 1506 (2013).
[47] R. D. Groot and P. B. Warren, Dissipative particle dynamics: Bridging the gap between atomistic and mesoscopic simulation, J. Chem. Phys. **107**, 4423 (1997).
[48] P. Espanol and P. Warren, Statistical mechanics of dissipative particle dynamics, Europhys. Lett. **30**, 191 (1995).
[49] J. H. Irving and J. G. Kirkwood, The statistical mechanical theory of transport processes. IV. The equations of hydrodynamics, J. Chem. Phys. **18**, 817 (1950).
[50] J. G. Kirkwood and F. P. Buff, The statistical mechanical theory of surface tension, J. Chem. Phys. **17**, 338 (1949).
[51] R. Mari, R. Seto, J. F. Morris, and M. M. Denn, Discontinuous shear thickening in Brownian suspensions by dynamic simulation, Proc. Natl. Acad. Sci. U.S.A. **112**, 15326 (2015).
[52] J. Comtet, G. Chatté, A. Niguès, L. Bocquet, A. Siria, and A. Colin, Pairwise frictional profile between particles determines discontinuous shear thickening transition in non-colloidal suspensions, Nat. Commun. **8**, 15633 (2017).